THE UNIVERSITY *of* EDINBURGH

Edinburgh Research Explorer

Geo-Characterization at selected accelerometric stations in Crete (Greece) and comparison of earthquake data recordings with EC8 elastic spectra

VERSITA

Central European Journal of **Geosciences**

Geo-Characterization at selected accelerometric stations in Crete (Greece) and comparison of earthquake data recordings with EC8 elastic spectra

Geoinformation Conference

A. Savvaidis[1]*, B. Margaris[1], N. Theodoulidis[1], V. Lekidis[1], Ch. Karakostas[1], C. Loupasakis[2], D. Rozos[2], P. Soupios[3], M-D. Mangriotis[4], U. Dikmen[5], Par. Tsangaratos[2], E. Kokinou[3], A. Vafidis[6], Th. Rondoyanni[2], I. Kalogeras[7], S. Koutrakis[7], A. Sarris[8], N. Papadopoulos[8]

1 Institute of Engineering Seismology and Earthquake Engineering (EPPO), Thessaloniki, Greece

2 Laboratory of Engineering Geology and Hydrogeology, Department of Geological Sciences, School of Mining and Metallurgical Engineering, National Technical University of Athens, Greece

3 Laboratory of Geophysics and Seismology, Department of Natural Resources and Environment, Technological Educational Institute of Crete, Chania, Crete, Greece

4 Institute of Petroleum Engineering, Heriot-Watt University, UK

5 Department of Engineering Geophysics, Engineering Faculty, Ankara University, Ankara, Turkey

6 Applied Geophysics Laboratory, School of Mineral Resources Engineering, Technical University of Crete, Greece;

7 Institute of Geodynamics, National Observatory of Athens, Greece

8 Laboratory of Geophysical-Remote Sensing & Archaeoenvironment, Institute for Mediterranean Studies, Foundation for Research & Technology Hellas, Greece

Abstract: To estimate the seismic response according to Eurocode (EC8) and almost all other national codes, site conditions have to be properly characterized so that soil amplification and the corresponding peak ground motion can be calculated.

In this work, different geophysical and geotechnical methods are combined in order to define the detailed ground conditions in selected sites of the Hellenic Accelerometric Network (HAN) in Crete. For this purpose, the geological information of the sites and shear wave velocity, calculated from surface wave measurements, is used. Additionally, ground acceleration data recorded through HAN have been utilized from intermediate depth earthquakes in the broader area of South Aegean Sea.

Using the recorded ground motion data and the procedure defined in EC8, the corresponding elastic response spectrum is calculated for the selected sites. The resulting information is compared to the values defined in the corresponding EC8 spectrum for the seismic zone that includes the island of Crete.

The comparison shows that accurate definition of ground type through geological, geotechnical and geophysical investigations is important. However, our current comparison focuses on the distribution of values rather than the absolute values of EC8-prescribed spectra, and the results should be considered in this context.

Keywords: geoinformation • earthquake hazard • Eurocode-EC8 • environmental protection • Crete

         © Versita Sp. z o.o.

*E-mail: alexandros@itsak.gr

1. Introduction

Given the impact on human losses, built environment and socioeconomic destruction from strong ground shaking, seismic risk mitigation is a primary objective of research activities in the fields of seismology and earthquake engineering. Well-known examples such as earthquakes in Mexico City in 1985 [1], Northridge in 1994 [2], Athens in 1999 [3], and Izmit and Duzce in 1999 [4], have illustrated that surface geology can drastically exacerbate damage. So-called site effects depend on geological conditions, both lithological and geomorphological, and may produce strong modifications in magnitude, frequency content and duration of earthquake ground motion. Since site effects may drastically increase the level of seismic hazard even in areas with moderate seismicity, their assessment becomes a major concern in seismic risk mitigation.

The methods which are generally considered as the most reliable for site effect estimation are site-specific and follow either an empirical or a numerical approach. The empirical-instrumental approach, originally proposed in [5], compares the spectral contents of the earthquake recordings obtained at the site of interest with a corresponding one obtained at a nearby rock sited station used as a reference site, using the so-called Standard Spectral Ratio (SSR). The numerical approach provides ground motion prediction based on a geophysical model of the site [6].

The empirical-instrumental approach requires a large number of recorded events for both active and reference stations, with a negligible distance between stations compared to the epicentral distance. This approach is not suitable where the amount of data is limited, for example in low seismicity areas. The numerical approach requires site surveys to provide a detailed soil model as a function of depth in order to constrain numerical results within the frequency range of engineering importance. The duration and cost of such surveys impose limitations for intensive application. As an alternative to assessing site effect, geo-characterization of a site might be used as a proxy because it is easier to extend to a large area and it does not need earthquake recordings.

The European and American seismic code regulations (Eurocode-EC8 and National Earthquake Hazards Reduction Program, NEHRP) include consideration of site effects through a simple site classification based on time-averaged shear wave velocity of the first 30 m (known as V_{S30}) and associated spectral shapes. However, although V_{S30} is widely used as a proxy to actual site conditions and site effects, it is often criticized because it may not capture fully the dominant physics of site amplification [7, 8].

Indeed, the response spectrum is the maximum response amplitude level at a given oscillator frequency. However, the simplicity of V_{S30} site classification and the relatively low cost of the background site survey has made the V_{S30} approach very popular. In particular, the approach became popular because until today no alternative combining cost effectiveness, simplicity and physical relevance to the underlying phenomena has been proposed.

To estimate the seismic action according to Eurocode (EC8), the soil amplification and the corresponding peak ground motion should be estimated. For this reason, a design spectrum using the ground type/soil category (S) and the peak ground acceleration (PGA) of the reference return period for the corresponding seismic zone and for the construction structural technical requirements have to be defined. The ground type is defined through geophysical or geotechnical parameters.

The appropriateness of average nationwide design specifications compared to regional specifications is often discussed for seismic hazard and its associated risk reduction. For instance, variations in the seismotectonic environment may significantly affect the spectral content of ground motion, resulting in elastic design spectra that differ from corresponding seismic code values. Such a deviation may come mainly from a lack of recorded seismicity in the statistical set used to prescribe seismic action in code provisions. Alternatively, geotechnical or geophysical methods used to characterize a site may lead to results that are not relevant to the soil type used in the seismic code. For the aforementioned reasons, it is vital that seismic code design spectral values are applied over regions appropriate to a specific seismotectonic environment; specified by actual regional seismic recordings and/or new results from improved geophysical or geotechnical characterization for a site.

In order to accomplish this, we present information and earthquake recordings for selected sites of the accelerometric network of Crete Island. This operates as part of the national Hellenic Accelerometric Network (HAN), and is maintained by the Institute of Geodynamics of the National Observatory of Athens (GEIN-NOA) and the Institute of Engineering Seismology and Earthquake Engineering (ITSAK-EPPO). The first installation of accelerometers in Greece on a national scale started in the early 1970's, while the regional network of Crete Island was deployed during the 1980's. Initially, analogue seismometers were deployed followed by low-resolution digital seismometers (after 2000). Since 2008, a denser state funded network was installed consisting of 36 digital (5 from GEIN-NOA and 15 from ITSAK-EPPO are 24-bit-high-resolutionsystems). To fully exploit the network it is necessary to characterize and document the recording

sites in terms of their near surface characteristics.

In the present work we improve the understanding of the relationship between near–surface geology (as defined from geotechnical mapping at the appropriate scale) and seismic shear wave velocity (V_s) and its variation with depth. We use in–situ geophysical measurements at selected strong motion stations. Both the empirical and numerical approaches are used in order to define the soil category from EC8. As shown in this study the differences between medium and large–scale maps along with the V_{S30} estimates are pronounced. Such information is critical to estimate the elastic spectrum by incorporating more realistic site conditions corresponding to in situ mapping and geophysical measurements. The recorded ground motion data from intermediate depth events in Crete and the surrounding area were used and the procedure defined in EC8 as followed to calculate the corresponding normalized response spectra for selected sites. These values are compared to those prescribed by the corresponding EC8 design spectrum for the seismic zone comprising the island of Crete. As a final outcome of this on–going work, our goal is to propose region specific elastic spectra for the seismic design of structures and for urban development planning will be proposed. These spectra are compared with Eurocode provisions and observed differences are highlighted to be taken into account for improving seismic design actions in the South Aegean area.

2.   Data and methodology

2.1.   Geo-characterization in Crete

In order to accomplish site characterization at the strong motion sites of the Hellenic Accelerometric Network in Crete, complementary geotechnical fieldwork took place. This work included detailed geological mapping of the thirteen strong motion sites under investigation, at a scale of 1:2000. In addition, the existing geotechnical and engineering geological data (e.g. the archives of the Institute of Geological and Mineral Exploration, the Central Public Works Laboratories and studies conducted by private geotechnical companies) were collected, evaluated and used to improve knowledge of the geotechnical characteristics of formations in the study areas.

After geological mapping, geophysical measurements were acquired in the vicinity (within 50m) of the nine selected strong-motion stations. The seismic methods of active source Multichannel Analysis of Surface Waves (MASW) and passive source Microtremor Array Measurements (MAM) were applied to provide information

about the V_{S30} for the areas under investigation.

From the available geophysical and geotechnical data, subsurface models were constructed for the selected sites where permanent strong motion stations of HAN are installed on Crete (Figure 1). These models were used as input information for a theoretical and experimental evaluation of the site effects.

2.2.   Horizontal elastic response spectra defined in EC8

In EC8, seven ground types (A to E and two special types S_1 and S_2) are prescribed, to account for the influence of local ground conditions on the seismic action. The types are defined either through a qualitative description of the corresponding stratigraphic profile or through quantitative parameters. These parameters are the average value of propagation velocity of S waves in the upper 30 m of the soil profile, V_{S30} at shear strain of 10^{-6} or less, the Standard Penetration Test blow count NSPT, or the undrained shear strength of soil, cU. For ground types S1 and S2, special studies for the definition of seismic action are required. For the other ground types (A to E), two types of elastic response spectra (Type–1 and Type–2) are prescribed depending on the surface–wave magnitude, M_s. If the earthquakes that contribute most to the seismic hazard defined for the site (for the purpose of probabilistic hazard assessment) have M_s greater than 5.5, Type–1 elastic response spectra is selected. For $M_s \leq 5.5$, Type–2 elastic response spectra is selected. It should be noted that Eurocodes allow a certain number of their classes and parameters to be defined through a National Annex specific for each EU country state. Hence, for Greece only Type–1 spectra are applicable (as defined in the corresponding Greek National Annex).

As seen in Figure 2(a), the typical horizontal elastic response spectrum shape consists of four sequential branches whose range is defined by their characteristic spectral periods T_B, T_C and T_D. T_B, T_C and T_D all depend on the ground type. The first branch starts from a seismic-zone dependent design ground acceleration value of $S \cdot a_g$ (at $T = 0$) and increases linearly up to a value of $2.5 \cdot S \cdot \eta \cdot a_g$, where S is a soil parameter whose value also depends on the ground type, and η is a structural damping correction factor with reference value $\eta = 1$ for 5% viscous damping. The second branch retains a constant value up to period T_C. The third branch decreases with one over the period, up to a value of T_D. Finally, the last branch continues decreasing inverse to the square of the period up to $T = 4$ sec. The EC8 shapes of Type–1 elastic response spectra for ground types A to E for Greece can be seen in Figure 2(b). Note that the Greek National Annex

Figure 1. The distribution of the HAN stations in Crete. The triangles and circles indicate the ITSAK/EPPO and the GEIN/NOA strong motion instruments, respectively. Circles of magenta color with a black outline indicate the epicenters of the earthquake events recorded.

adopts the values of T_B and T_C recommended in EC8, but prescribes a value of $T_D = 2.5$ sec for all ground types (instead of the EC8-recommended value of $T_D=2.0$ sec).

Finally, it should be noted that a vertical elastic response spectrum, as well as the corresponding design spectra for elastic analysis of structures, are prescribed in EC8 (both based on similar concepts as those of the horizontal elastic response spectrum described above), but their detailed presentation falls beyond the scope of the present paper.

It is well known that in order to define elastic response spectra according to the EC8 seismic code, ground type must be defined (e.g. A, B, C, D, E) as must its corresponding soil factor, S; spectral amplification is selected. Among the parameters used to quantitatively characterize ground type is the average shear wave velocity of the upper 30 m geologic layers, known as the V_{S30} value. In this work the geo-characterization of strong motion sites in Crete Island led to V_{S30} value estimates that can be used to construct elastic response spectra according to the EC8 seismic code. These elastic response spectra can be compared with actual recorded response spectra after the latter has been properly normalized. Especially for the design or seismic assessment of long period structures (such as high-rise buildings, bridges, flexible industrial structures etc.) there is still a need to

investigate the adequacy of the code-prescribed spectral shapes, especially for the case of intermediate depth earthquakes, whose frequency content is rich in the medium to long period range (¿1.5sec). As a final check, a direct comparison between EC8 elastic spectral shapes and observed spectral shapes was attempted. Such a comparison may prove the sufficiency or insufficiency of seismic actions proposed for the EC8 for selected sites or regions. If they are not appropriate the elastic response spectra could by modified and corrected so that they more closely correlate to the recorded ground motion, thus proposing more realistic design seismic actions. In this work, based on selected recordings for selected geo-characterized strong motion stations in Crete for which ground motion recordings were available, the aforementioned approach was applied as part of an ongoing process. The same approach could be applied to the rest of strong motion stations at a later stage.

3. Geological & geotechnical setting of the accelerograph foundation conditions

The detailed geological mapping around the HAN strong motion sites proved that the common practice of using
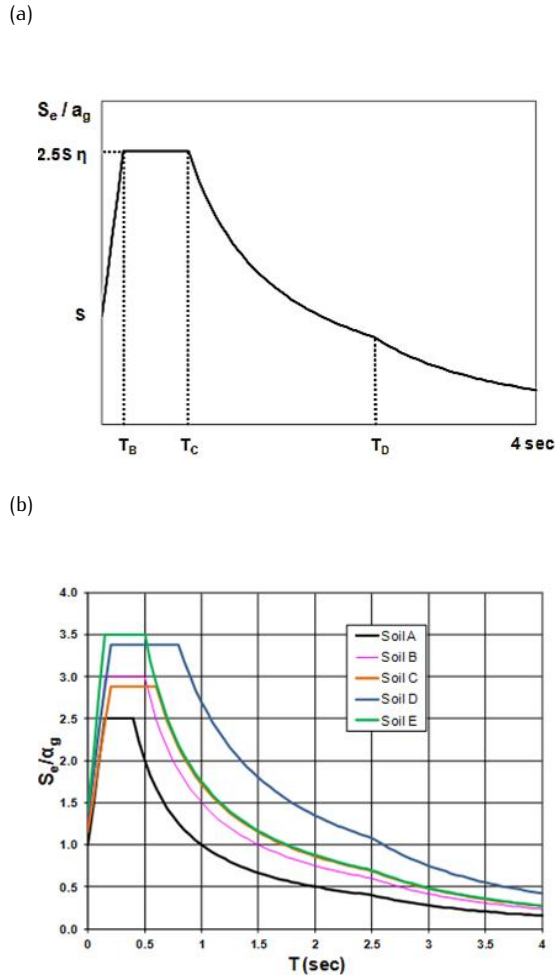
(a)

(b)

Figure 2. (a) Shape of the EC8 elastic response spectrum; (b) Type-1 elastic response spectra for ground types A to E for Greece.

medium–scale geological maps (e.g. the IGME maps with 1:50,000 scale) for the geo–characterization of sites is not always precise. At several sites, such as CHN2, PLC1, RTH1, SIVA, AGNA, AGN1 and ZKR, new certain or probable faults were identified very close to the stations (Figure 3). These data highlighted new targets for the geophysical research as the location and orientation of the tectonic setting provided new perspective on the models of seismic wave prorogation. For example, at the ZKR station instead of the phyllites indicated by the IGME geological map [9], a completely different geological structure was identified. The station is located over a 15 m thick Triassic limestone tectonic nappe thrusted over Permian–Triassic phyllites (Figure 3). This completely different and complex geological structure affects the propagation

of seismic waves across the over–thrust surface and therefore the mechanical characteristics of the formations are intensively downgraded.

Besides the new data concerning tectonic structure, geological mapping revealed variations that alter the ground type/soil category of the foundation formations (Table 1). In particular, substantial variations were observed at the CHN2, HER2, HER3, and AGN1 stations. The CHN2 accelerometric station, located in the center of Chania, is founded on marly conglomerates of Neogene age with alternating layers of marly limestone and white to yellowish marls according to the small–scale mapping in this study (Figure 3). The total thickness of the formation appears to reach several tens of meters and can be categorized as A–class, rock–like geological formations (Eurocode 8, EN 1998). However, according to the IGME mapping the station is supposed to be founded on loose marly sandstones [10], ground type/soil–category C. At the HER2 accelerometric station located at the historical center of the Heraklion city, the mapping as well as the available geotechnical drill profiles revealed the existence of a 10 to 15 m thick layer of historical and recent deposits over the stiff marls (Figure 3) instead of the marls indicated by the IGME geological map [11]. This information downgrades the ground type/soil category (Eurocode 8, EN 1998) from B to D. In contrast, the category of the foundation formations of the HER3 station is upgraded from D, or even worse from S2, to B. This is because the small–scale mapping proved that HER3 is sited over thick Neogene marls (Figure 3) instead of the previously–thought loose coastal sands [11] which would have high liquefaction potential. Another station with considerable alteration in the ground type/soil category is the AGN1 station, which according to the IGME maps is founded over limestone [12] but according to the detailed geological mapping is more likely to have a few meters of loose alluvial deposits laying over the limestone. This changes its classification to E instead of A.

The disagreement in the type of foundation formations described above does not imply that these maps are of bad quality. On the contrary, it is a reasonable disagreement resulting from the combined complexity of the geological structure and the low scale of the IGME maps.

Comparing the category types defined from geophysical data, described in the next sections, with the one defined from the detailed mapping, two very interesting findings come out. Firstly, on sites with Neogene rock–like geological formations, such as marly conglomerates, the calculated V_{S30} values downgrade the ground type from A to B (Table 1 – CHN2 and AGNA). Therefore, the ground type/soil–category of these formations must not be overestimated even though they appear to be sited
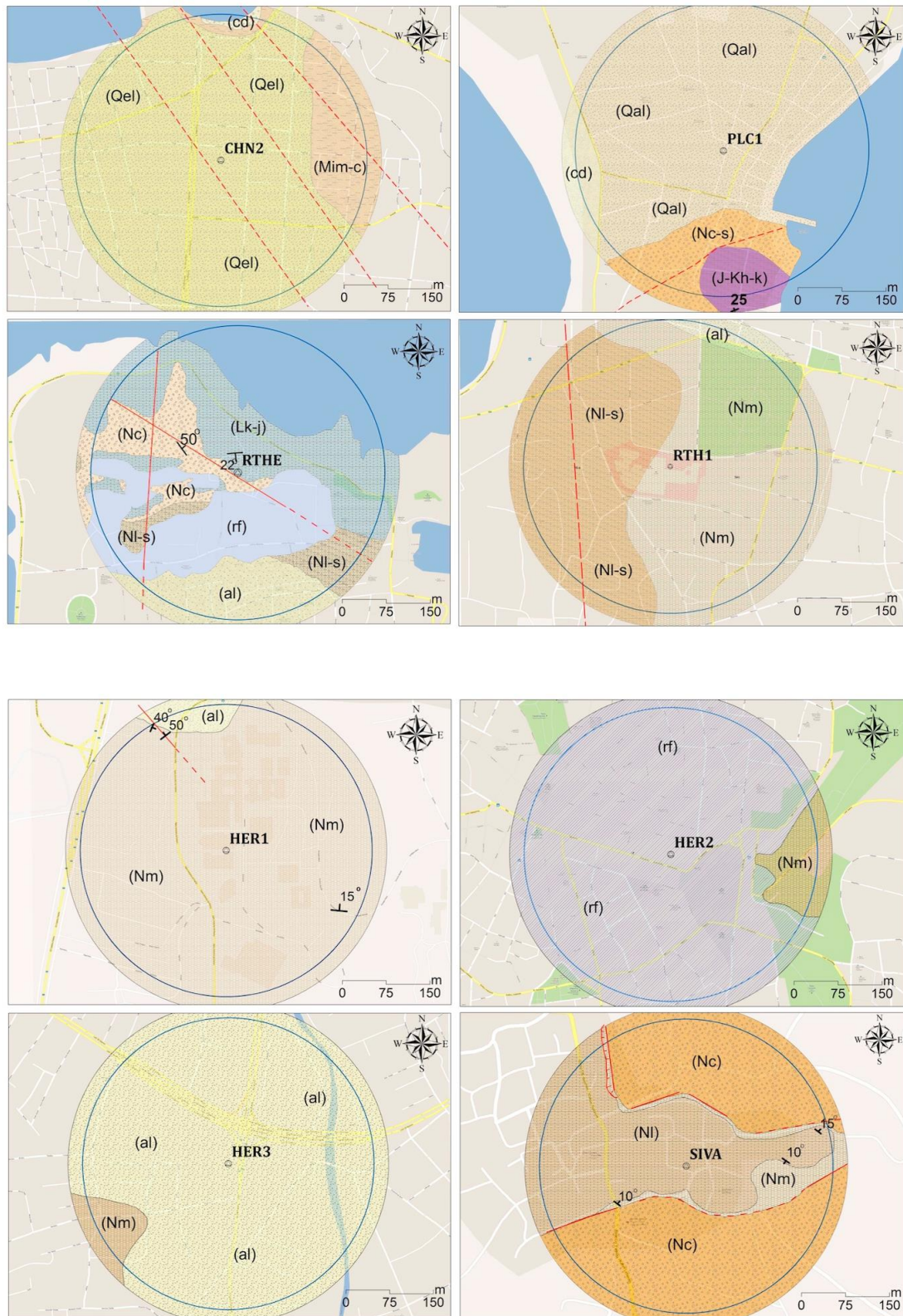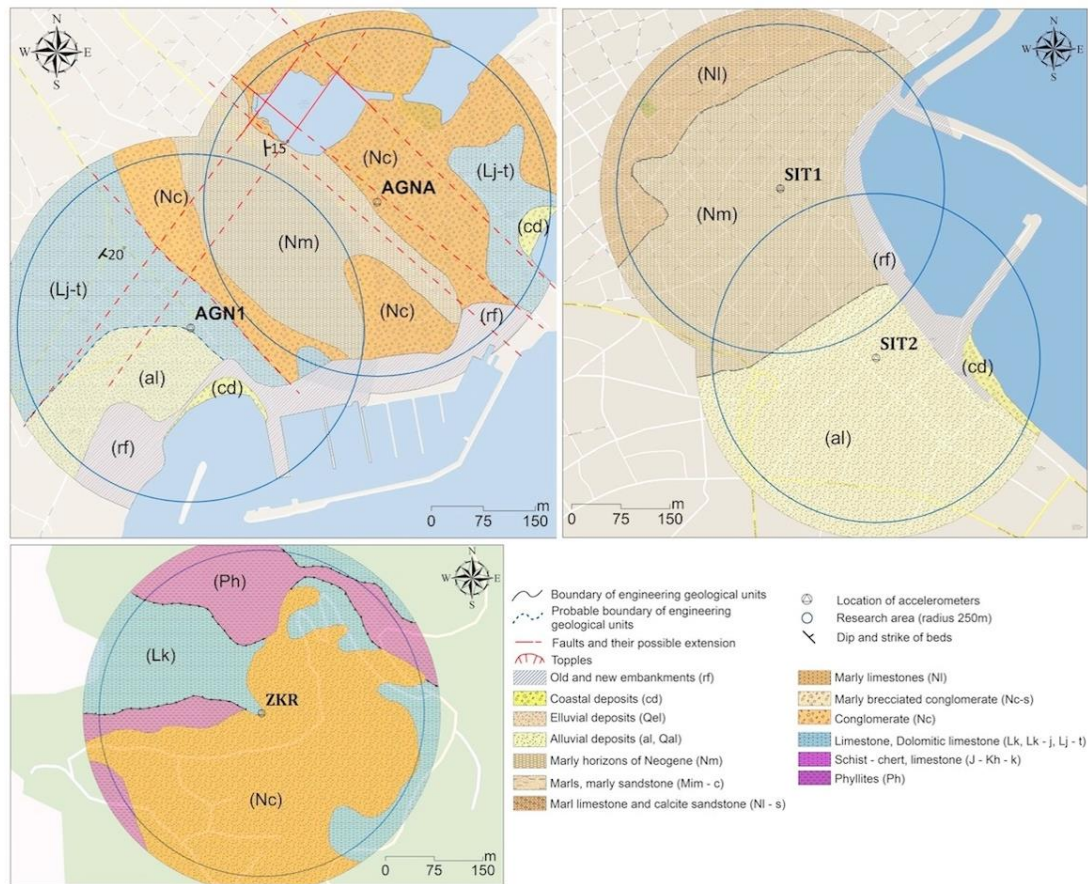
Figure 3. Geological maps of the strong motion stations.

on rock–like formations. The second finding concerns the sites with shallow depth, less than 10 m, with loose to medium density deposits (HER2, AGN1, SIT2). According to EC8 and based on the description of the stratigraphic profile, the ground type is underestimated. As presented in Table 1, the category estimated by the geophysical data is upgraded (to B for HER2 and AGN1 from D and E respectively, and to C from D for SIT2) depending on the shear wave velocity of the underlying formations.

4.   Geophysical data and results

A comprehensive series of seismic surveys, including MASW and MAM testing (e.g. [13, 14]), were completed in December 2012 in order to determine the V_s profiles at 9 strong motion stations in Crete. These surveys were designed to deduce the ground type conditions based on the EC8 classification. Instrumentation consisted of a 24–channel seismograph with 4.5 Hz (low frequency) vertical component geophones, and a 7 kg sledge–hammer, which was used as the active seismic source for MASW. Figure 4 shows a picture from the MASW seismic tests carried out at station AGNA. Different geophone spacing (dx) layouts and various source–receiver offsets (0–65 m) were acquired at each location to assess the scale of any possible lateral heterogeneity and limitations due to the signal–to–noise (S/N) ratio. All seismic data were recorded with a sampling interval (dt) of 2 ms for a total record length of 4 seconds for MASW and 20 minutes for MAM. More that 15 shots were acquired for the MASW surveys to reduce the environmental noise. We discuss one station, HER1, located in the city of Heraklion. Results for the remaining stations are presented in the Appendix, and the corresponding V_{S30} values along with the corresponding soil category are presented in Table 1.

Table 1. The foundation formations according to the medium scale geological maps of IGME and the small-scale maps created within the framework of the current study. The corresponding ground type/soil categories are presented. The ground type and the corresponding V_{S30} values as a result of the geophysical prospecting are also shown as described in the next section. Foundation formations or soil categories that change from one ground type categorization method to the other are highlighted in red.

	Medium-scale maps		Small-scale map		Geophysical results	
Station	Station foundation formations	Ground – type	Station foundation formations	Ground – type	V_{S30}	Ground – type
CHN1					903	A
CHN2	Loose marly sandstones	C	Stiff marly conglomerate and marly Limestones	A	578	B
PLC1	Loose alluvial deposits	D	Loose alluvial deposits	D		
RTH1	Clayey marls	B	Clayey marls	B		
RTHE	Limestones and dolomites	A	Limestones and dolomites	A		
HER1	Marls	B	Marls	B	378	B
HER2	Marls	B	Recent and historic deposits	D	413	B
HER3	Coastal loose sands	D or S2	Marls	B		
SIVA	Conglomerates, sandstones and marls	B	Marls and Marly sandstones	B		
AGN1	Limestones and dolomites	A	Loose alluvial deposits over limestones	E	476	B
AGNA	Marly conglomerate	A	Marly conglomerate	A	476	B
SIT1	Marls	B	Marls	B	416	B
SIT2	Loose alluvial deposits	D	Loose alluvial deposits	D	242	C
ZKR	Phyllites	A	Overthrusted limestones	A	871	A

At site HER1, 1 m and 3 m geophone spacing were used for both MASW and MAM seismic methods. For the MASW data, shot gathers with the highest S/N ratio were selected and their corresponding frequency–wavenumber (f–k) spectra were computed, using the phase–shift algorithm [15]. In all stations, a minimum of 20 m was used for the source–receiver distance in order to reduce near–field effects. For the MAM data, the entire receiver array was used for the f–k spectra computation. Two seismic shot gathers are presented in Figure 5.

After computing the phase velocity–frequency map from the phase–shifting transformation, we selected the dispersion curve, which is defined as the Rayleigh wave phase velocity as a function of frequency. The dispersion curve can either be automatically or manually picked. In this study, we used automatic picking to estimate the maximum energy point for each frequency line in the phase velocity–frequency map, but also used manual quality control to ensure that the maximum values did not correspond to higher modes, in which case the values were picked manually.

All processing of the dispersion curves was performed using the software SeisImager S/W [16]. The MAM and MASW dispersion curves, which showed good agreement with each other, were combined via averaging and smoothing in order to produce a single dispersion curve for the V_s inversion for each station. The dispersion curve had a low–frequency cutoff determined from the maximum array length D using the relationship $\lambda_{max} < 2D$, whereas the high–frequency cutoff was determined from the relationship $1/\lambda_{min} = 1/dx$, where dx is the receiver spacing [17].

Figure 6 shows the phase velocity spectrum for HER1 for the array with $dx = 3$ m, for MAM data. Figure 7 shows the MASW phase velocity spectrum for the same receiver array for 65 m offset. The dispersion curve corresponding to the array with $dx = 1$ m was not used as it contains too much lateral heterogeneity from shallow layers.

For V_s inversion of the dispersion curves, we used the Neighborhood algorithm [18], which is available from the open source software geopsy [19]. Inversions were performed using five model scenarios with an increasing number of layers starting from one uniform layer over half–space, up to five layers over half–space. Input models assumed: (a) constant density of 2000 kg/m^3 for uniform layers and 2700 kg/m^3 for the half–space, (b) V_p ranging from 200 to 5000 m/s, (c) a V_s range of 150 to 3500 m/s, and (d) upper and lower bounds for the thicknesses assigned from the λ_{min} and λ_{max} values, with layer thickness increasing with depth by using
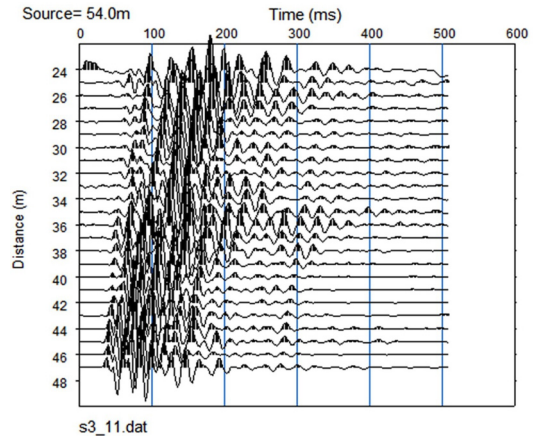
Figure 4. Receiver array set-up for MASW and linear MAM surveys at station AGNA. Geophone spacing of 3 m is shown.

(a)

(b)

Figure 5. (Shot gathers for stations (a) CHN2 (b) HER1.

depth ranges based on a geometrical progression of the thickness over a fixed depth range in a 1D structure [20]. 0 standard deviation (s.d) was assumed since no s.d. is provided by SeisImager. The computed misfit is given by the expression $misfit = \sqrt{\sum_{i=1}^{n_t} \frac{(x_{di} - x_{ci})^2}{x_{di}^2 n_f}}$, where n_f is the number of frequency samples considered, x_{ci} is the velocity of the calculated curve at frequency f_i, and x_{di} is the velocity of the data curve at frequency f_i The best model was selected based on minimising misfit, and the corresponding corrected Akaike estimate [21, 22].

Table 2 shows the misfit calculated by the Neighborhood algorithm inversion results misfit, as well as the corrected Akaike estimates [21, 22] for HER1. The corresponding V_s profile producing the smallest Akaike estimate (1 uniform layer over half–space model) for the Neighborhood algorithm is shown in Figure 8, for a misfit range of up to 0.035. The final V_s profile for HER1 is shown in Table 3, which corresponded to a V_{S30} value of 377.6 m/s. This results in a category of B for the site based on EC8 soil classification.
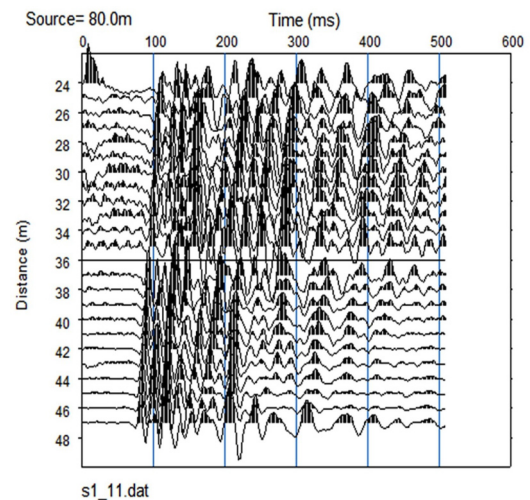
5. Comparison of spectral shapes

In the following, comparisons are made between elastic response spectra according to EC 8 and observed spectral values, which have been recorded by accelerographic instruments installed in the Chania, Heraklion, Agios Nikolaos and Sitia sites in Crete. In these comparisons the observed spectral values were derived from accelerograms, which have been recorded by instruments triggered by strong intermediate
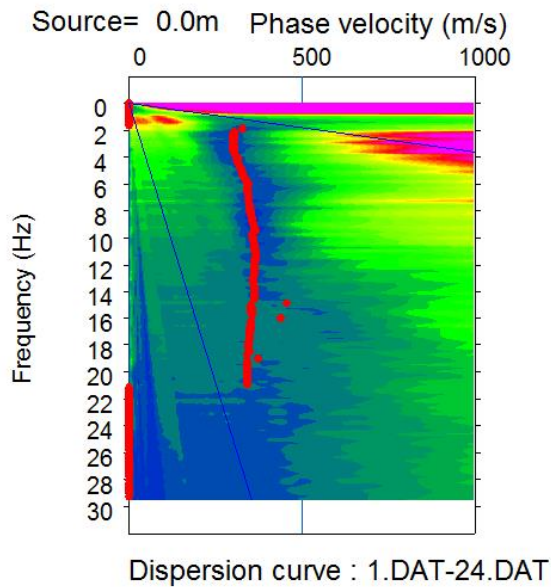
Figure 6. Phase velocity spectrum for HER1 from MAM data. Automatically picked dispersion curve is shown with red dots.
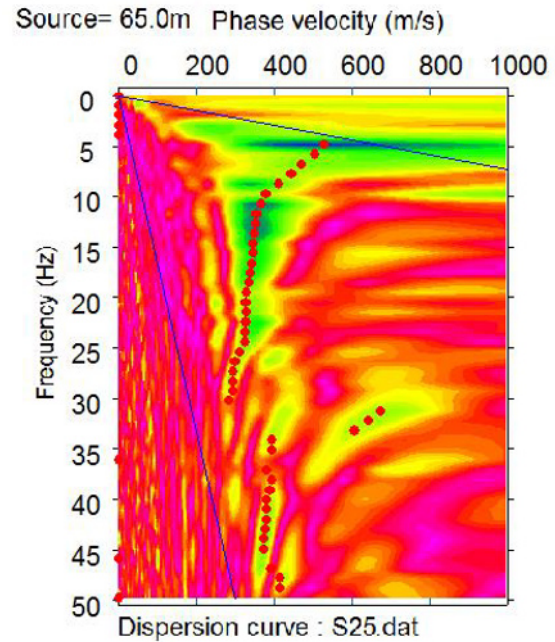
Figure 7. Phase velocity spectrum for HER1 from MASW data for 65 m offset. The manual selection of the automatically picked dispersion curve is shown with red dots. Only data from 5-30 Hz was used in further inversion.

Table 2. Neighborhood results showing model number of layers over half-space (LHS), degrees of freedom (DoF), minimum misfit estimates and corrected Akaike estimates (AICc). nf corresponds to number of frequency points in the dispersion curve.

Model	DoF	Misfit	AICc
1LHS	7	0.016022	−96.1462
2LHS	11	0.008759	−94.1555
3LHS	15	0.009786	−59.5519
4LHS	19	0.008842	0.608871
5LHS	23	0.008863	189.6749
6LHS	27	0.012216	inf
nf		28	

depth earthquakes (hypocentral depths ¿ 50 km). In Table 4, INDEX (used in Figure 9 to denote different recordings), the code station name (NAME), the geographical coordinates of the accelerographic stations (LAT, LON), the origin time (following the YYMMDDHHMMSS format) of the earthquake event (ORIGIN TIME), the geographical coordinates (EPLAT, EPLON) of the earthquake hypocenter, the depth of the hypocenter (DEP), the earthquake magnitude (MAG), and the instrument type (INSTR) are given.

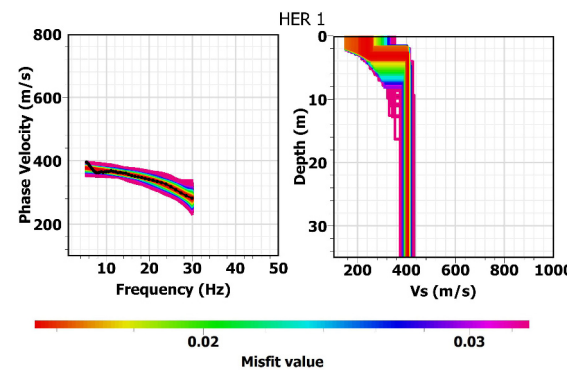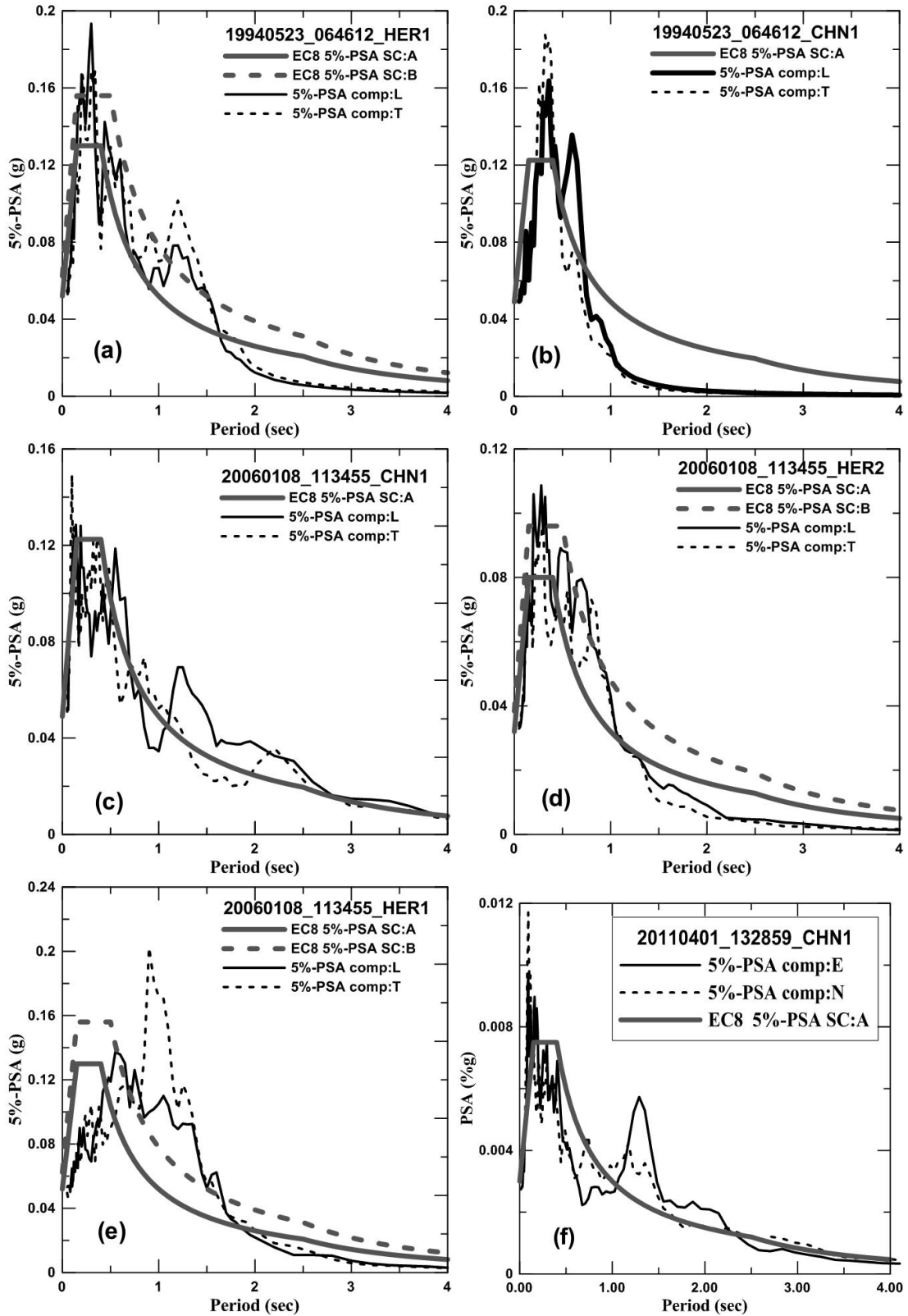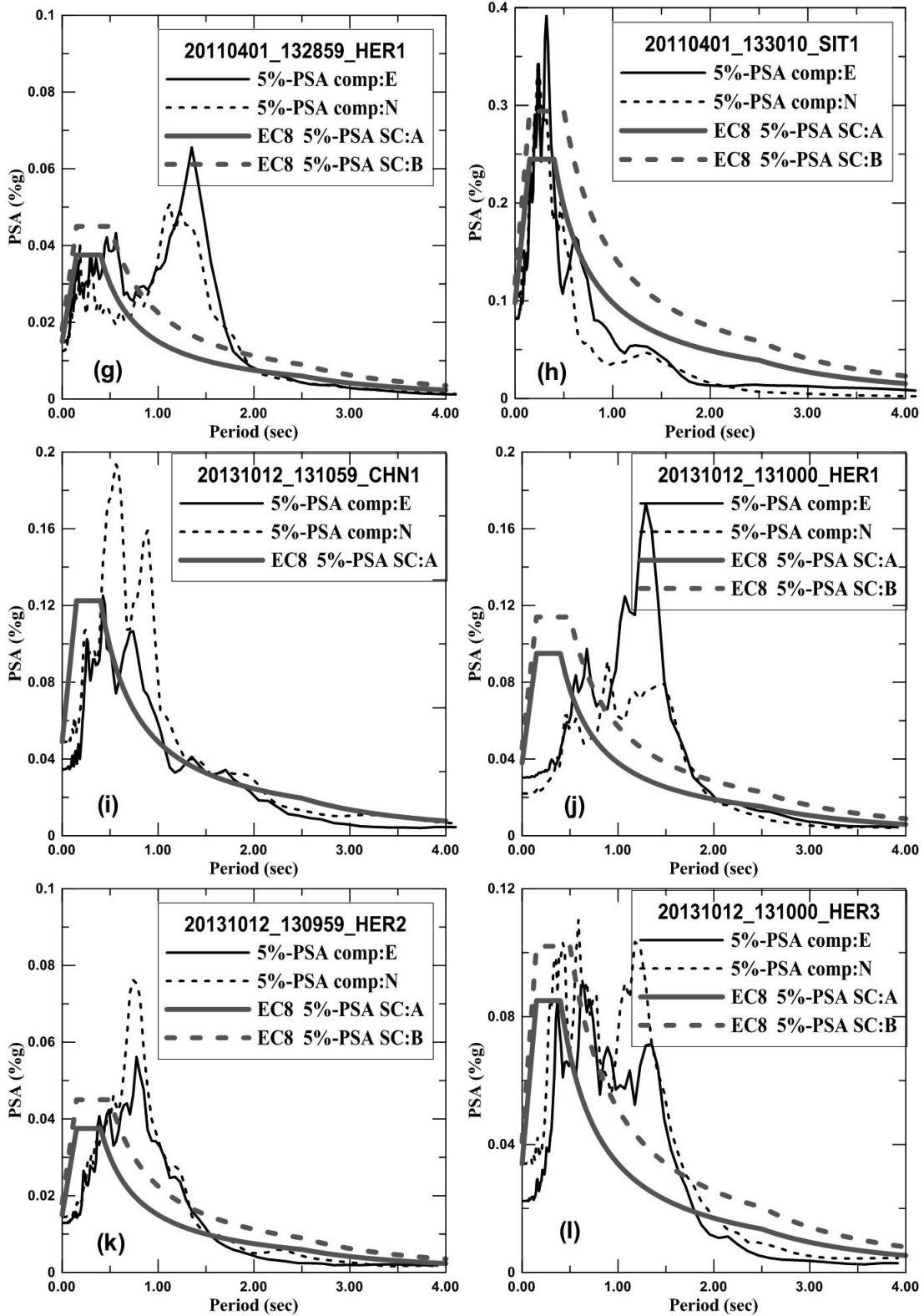In Figure 9(a) – Figure 9(n) the acceleration response

Figure 8. Inversion results for HER1 using one uniform layer over half-space. The left plot shows the model dispersion curve vs. the calculated dispersion curve (black). The right plot shows the corresponding V_s profile for models with misfit less than 0.035.
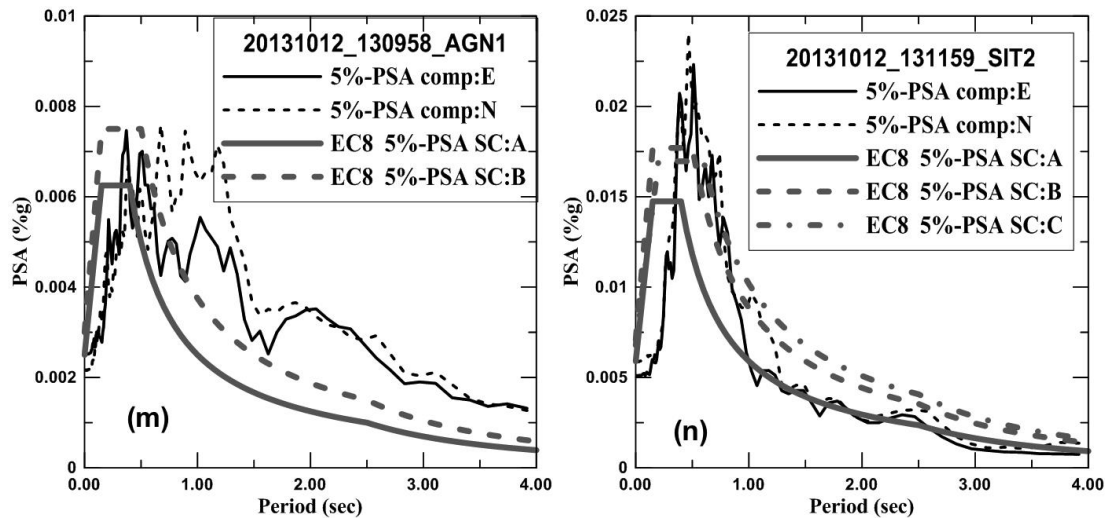
Figure 9. Observed and calculated acceleration response spectra for different stations and earthquake events as described in Table 4. The observed data are denoted with black color continuous and dashed lines for Longitudinal or East, and Transverse or North components, respectively. The theoretical elastic spectrum prescribed in EC8 (PGA-scaled) is presented for different ground type conditions, A, B and C, denoted with grey continuous, dashed and dotted dashed lines, respectively.

Table 3. Description of best V_s model for HER1.

Thickness	V_S (m/s)	V_{S30} (m/s)	Soil Category (EC8)
3.2	239	377.6	B
inf	406		

spectra from the accelerograms described in Table 4 are presented calculated for 5%-damping and for the two horizontal components separately (L–longitudinal and T–Transverse, or E–East and N–North) of the seismic motion. The observed spectral values are compared to the elastic response spectra scaled for various PGA's corresponding to actual recordings and for different soil categories (SC) according to EC8 (A: continuous line, B: dashed line and C: doted dashed line).

The selected PGA values, where the EC8 elastic response spectra are anchored, correspond to the peak ground values of the recorded accelerations for each station. For the stations examined in this paper, the ground type (soil category) is defined in Table 1 and the ones presented is SC–A for all sites. For those sites that geophysical data that do not exist we present the SC from A up to the one derived from small–scale geological mapping.

In most cases, the observed spectral values are not in agreement with the EC8 spectral shapes mainly because of more periods between 0.5 and 2.5 s. The only exception is at the Sitia site, for stations SIT1 and SIT2, where the observed spectral values are in good agreement with the normalized corresponding EC8 ones (Figure 9(h) and Figure 9(n)). For station Chania (CHN1), the observed data deviate from those of the EC8 for a wide period range between 0.5 sec and about 2.5 sec. For the recording 19940523_064612_CHN1 (Figure 9(b)), the observed lack of energy for periods greater than about 1sec is probably due to the low resolution of the analog instrument installed (SMA-1, see Table 4). The Heraklion city stations HER1, HER2 and HER3 (Figures 9(a), 9(d), 9(e), 9(g), 9(j), 9(k) and 9(l)) show large deviations in the compared spectral shapes, especially for periods 0.8 sec to 1.8 sec, in agreement with results of previous work [23–25]. For recordings 19940523_064612_HER1 (Figure 9(a)) and 20060108_113455_HER2 (Figure 9(d)), the observed lack of energy for periods greater than about 1 sec is probably due to low resolution analog (SMA-1) and digital SSA-2 (12 bits) instruments (see Table 4). Finally, at the AGN1 accelerographic station, the recorded spectral shapes completely deviate from those of the EC8 normalized spectral curves and for a wide period range from 0.6 s to 4.0 s. To use the EC8 spectra when designing tall or/and flexible structures especially, the effects of intermediate–depth earthquakes (like the Kythera 2006 earthquake, which was the first of this type recorded by several HAN instruments) should therefore be

Table 4. The accelerographic stations and the earthquake parameters of the strong motion records utilized for the calculation of observed spectral values. Groups with the same color denote the same earthquake event.

INDEX	NAME	LAT	LON	ORIG. TIME	EPLAT	EPLON	DEP	MAG	INSTR.
(a)	HER1	35.3177	25.1022	940523064612	35.5409	24.6968	68	6.1	SMA-1
(b)	CHN1	35.517	24.0208	940523064612	35.5409	24.6968	68	6.1	SMA-1
(c)	CHN1	35.517	24.0208	060108113455	36.1853	23.4037	67	6.7	CMG5TD
(d)	HER2	35.3379	25.1356	060108113455	36.1853	23.4037	67	6.7	SSA-2
(e)	HER1	35.3177	25.1022	060108113455	36.1853	23.4037	67	6.7	CMG5TD
(f)	CHN1	35.517	24.0208	110401132910	35.6432	26.5643	63	6.0	CMG5TD
(g)	HER1	35.3177	25.1022	110401132910	35.6432	26.5643	63	6.0	CMG5TD
(h)	SIT1	35.2080	26.1050	110401132910	35.6432	26.5643	63	6.0	QDR
(i)	CHN1	35.517	24.0208	131012131153	35.5042	23.2773	65	6.4	CMG5TD
(j)	HER1	35.3177	25.1022	131012131153	35.5042	23.2773	65	6.4	CMG5TD
(k)	HER2	35.3379	25.1356	131012131153	35.5042	23.2773	65	6.4	CMG5TD
(l)	HER3	35.3296	25.1065	131012131153	35.5042	23.2773	65	6.4	CMG5TD
(m)	AGN1	35.1880	25.7160	131012131153	35.5042	23.2773	65	6.4	CMG5TD
(n)	SIT2	35.2059	26.1070	131012131153	35.5042	23.2773	65	6.4	CMG5TD

properly examined. That is, the EC8 normalized spectral shape does not satisfactorily describe the complexities in the medium range (0.5 sec¡T¡2.5 sec) periods that characterizes recordings of this type of earthquake, at least for the majority of the stations examined in this paper. An exception is the Sitia accelerographic stations (SIT1, SIT2), where EC8 normalized spectral shapes encompass observed spectral values, indicating therefore the possible absence of any site effect that may be present in the rest of the examined sites. A greater number of recordings of intermediate-depth earthquakes in Greece would help to improve EC8 as they were not considered at all when creating it.

6. Discussion and conclusions

We present steps for the calibration of the elastic spectra described in EC8 based on site geo-characterization defined by geological, geotechnical and geophysical data. It is very important to properly define the ground type at each site in order to suitably calibrate the corresponding code prescribed spectra, and to propose appropriate modifications to the EC8 spectral shapes to improve

seismic design actions. The current work has focused on the shape, rather than the absolute values of EC8-prescribed spectra, and the conclusions derived herein should be considered in this context.

Geological, geotechnical and geophysical investigations should be combined to accurately identify the ground type, or even its corresponding uncertainty. The detailed geological mapping around the thirteen strong motion stations of Crete in this study provide crucial information on the ground type/soil category of the foundation formations. These data, enriched by geophysical surveys, provide important information for the geo-characterization of sites which can be maximized by targeted geotechnical drilling.

It is evident from this study that the instrument's resolution may play an important role in realistically detecting low-amplitude, long period ground motion. The persistence of medium to long period (0.5 sec - 2.0 sec) spectral amplitudes that surpass the corresponding normalized EC8 elastic spectra is an indication of significant divergence of observed data from seismic actions proposed by the code. This difference may be due either to source effects or to a combination of source, path and site effects. Additional work based on observed and synthetic data

may help to shed light on this complex phenomenon.

More specific quantitative comparisons with the EC8 elastic spectral shapes prescribed for the studied sites will be possible when recordings from stronger earthquake events are available or when well-documented synthetic ground motion is provided. Additionally, more sites of the Hellenic Accelerometric Network need to be investigated and geo-characterized to allow for improved comparative evaluations between the code seismic actions and observed acceleration spectra. These may show that regional conditions for the area of Crete Island are more appropriate than national ones. These results will help to improve urban planning in the seismically active zone of the South Aegean within the context of seismic risk mitigation.

Acknowledgements

References

[1] Chavez-Garcia F. J and Bard P-Y, Site effects in Mexico city eight years after the September 1985 Michoacan earthquakes, *Soil Dynamic and Earthquake Engineering* 13, 1994, 229-247

[2] Field E. H., Johnson P. A., Beresnev I. A. & Zeng Y., Nonlinear ground-motion amplification by sediments during the 1994 Northridge earthquake, *Nature* 390, 1997, 599-602 doi:10.1038/37586

[3] Assimaki D., Gazetas G. and Kausel E., 2005, Effects of Local Soil Conditions on the Topographic Aggravation of Seismic Motion: Parametric Investigation and Recorded Field Evidence from the 1999 Athens Earthquake, *Bulletin of the Seismological Society of America* 95, 3, 2005, 1059-1089, doi: 10.1785/0120040055

[4] Sadik Bakir B., Sucuoğlu H. and Yilmaz T., An Overview of Local Site Effects and the Associated Building Damage in Adapazari during the 17 August 1999 İzmit, *Earthquake Bulletin of the Seismological Society of America* 92, 2002, 509-526

[5] Borcherdt R. D., Effects of local geology on ground motion near San Francisco Bay, *Bull. Seism. Soc. Am.* 60, 1970, 29-61

[6] Komatitsch D., Liu Q., Tromp J., Süss P., Stidham C. and Shaw J. H., Simulations of Ground Motion in the Los Angeles Basin Based upon the Spectral-Element Method, *Bulletin of the Seismological Society of America* 94, 2004, 187-206

[7] Castelarro S., F. Mulargia, and Luigi Rossi P., V_{S30}: Proxy for site amplification?, *Seism. Res. Letters* 79, 4, 2008, 540-543

[8] Assimaki D., W. Li, J. H. Steidl, and Tsuda, K., Site amplification and attenuation via downhole array seismogram inversion: A comparative study of the 2003 Miyagi-Oki aftershock sequence, *Bull. Seism. Soc. Am.* 98, 2008, 301-330

[9] Institute of Geology and Mineral Exploration-I.G.M.E., Geological map of Greece-Ziros Sheet, Scale 1:50.000, Athens, 1959

[10] Institute of Geology and Mineral Exploration-I.G.M.E., Geological map of Greece-Chania Sheet, Scale 1:50.000, Athens, 1971

[11] Institute of Geology and Mineral Exploration-I.G.M.E., Geological map of Greece-Heraklion Sheet, Scale 1:50.000, Athens, 1996

[12] Institute of Geology and Mineral Exploration-I.G.M.E., Geological map of Greece-Agios Nikolaos Sheet, Scale 1:50.000, Athens, 1987

[13] Park C. B., Miller R. D., and Xia J., Multichannel analysis of surface waves, Geophysics 1999, 64, 800-808, 1999

[14] Louie J. N., Faster, Better: Shear wave velocity to 100 meters depth from refraction microtremor analysis, *Bull. Seismol. Soc. Am.* 91, 2, 2001, 347-364

[15] Dal MoroG., Pipan M, Forte E., and Finetti I., Determination of Rayleigh wave dispersion curves for near surface applications in unconsolidated sediments, et al, SEG Annual Meeting 2003

[16] Windows Software for Analysis of Surface Waves – SeisImager S/WTM (http://www.geometrics.com), October 2009

[17] Socco L. V., and Strobbia C., Surface-wave method for near-surface characterization: a tutorial, Near Surface Geophysics, 2004, 165-185

[18] Whatelet M., Array recordings of ambient vibrations: surface-wave inversion, PhD Diss., Liége University, 161, 2005

[19] Open source software for geophysical research and applications (http://www.geopsy.org/)

[20] http://www.geopsy.org/man/gpdepths.html

[21] Savvaidis A., Ohrnberger M., Wathelet M., Cornou C., Bard P.-Y. and Theodoulidis N., 2009, Variability Analysis of Shallow Shear Wave Velocity Profiles Obtained from Dispersion Curve Inversion considering Multiple Model Parameterizations. SSA meeting, Poster 54, Monterey, USA

[22] Di Giulio, G., Savvaidis, A., Ohrnberger, M., Wathelet, M., Cornou, C., Knapmeyer-Endrun, B., Renalier, F., Theodoulidis, N., and Pierre-Yves Bard, Exploring the model space and ranking a best class of models in surface-wave dispersion inversion: Application at European strong-motion sites, GEOPHYSICS May 2012, 77, 3, B147-B166

[23] Skarlatoudis A. A., C. B. Papazachos, B. N. Margaris, Ch. Papaioannou, Ch. Ventouzi, D. Vamvakaris, A. Bruestle, T. Meier, W. Friederich, G. Stavrakakis, T. Taymaz, R. Kind, A. Vafidis, T. Dahm & the EGELADOS group, Combination of strong-and weak-motion recordings for attenuation studies: The case of the January 8, 2006 Kythera intermediate-depth earthquake, *Bull. Seism. Soc. Am.* 99, 2009, 694-704

[24] Boore D. M., A. A. Skarlatoudis, B. N. Margaris, C. B. Papazachos and Ch. Vendouzi, Along-Arc and Back-Arc Attenuation and Source Spectrum for the Intermediate-Depth 18 January, 2006, M 6.7 Kythera, Greece, Earthquake, *Bull. Seism. Soc. Am.* 99, 2009, 2410-2434

[25] Skarlatoudis A. A., C. B. Papazachos, B. N. Margaris, Ch. Ventouzi, I. Kalogeras and the EGELADOS group, Ground motion prediction equations of intermediate-depth earthquakes in the Hellenic arc, southern Aegean subduction area, *Bull. Seism. Soc. Am.* 103, 2013, 1952-1968

[26] Mastrolorenzo G., Profili di velocita V_s nell'abitato di Chania, Creta, Tesi di laurea, Universita degli Studi della Basilicata, Italy, 107 (in Italian), 2004

[27] Papadopoulos, H., Experimental and theoretical study of the local site-effect amplification using microtremor recordings and field geophysical measurements, Ph.D. Thesis, Geophysical Laboratory, Aristotle Univ. Thessaloniki, 411 (in Greek), 2013

Appendix A

In this appendix, the V_s inversion results for the remaining stations in Crete are presented for surface wave MASW and MAM testing during the December 2012 field expedition. V_s profiles were produced for stations HER1 (shown also in the main text), HER2, SIT1, ZKR, AGNA, AGN1, SIT2, and CHN2. No inversion was carried out at station HER3, for which the fundamental mode could not be identified because the phase velocity spectrum was dominated by a mixture of higher modes. In addition to the sites tested, the shear wave velocity profile for station CHN1 is also presented using the dispersion curve derived by [26]. For processing of both the dispersion curves and the V_s inversion we followed the steps presented in the main text for station HER1. The best V_s models (i.e. those with the smallest corrected Akaike value [21, 22]) are shown in Figure A.1 – Figure A.9 along with the experimental and model dispersion curves. Table A.1 summarizes the V_s profile at each station for the model with the smallest corrected Akaike value.
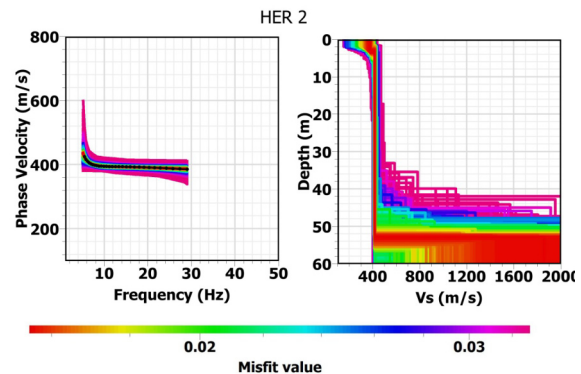

Figure A.1. Inversion results for HER2 using 2 layers plus half-space. Left plot shows the model dispersion curve vs. experimental dispersion curve (black), whereas right plot shows the corresponding V_s profiles for models with misfit less than 0.035.